Agglomeration and Adhesion Free Energy of Paracetamol Crystals in Organic Solvents

Eva M. Ålander and Åke C. Rasmuson
Dept. of Chemical Engineering and Technology, Royal Institute of Technology, SE-100 44 Stockholm, Sweden, 11267

DOI 10.1002/aic.11267
Published online August 28, 2007 in Wiley InterScience (www.interscience.wiley.com).

The agglomeration of paracetamol during crystallization in different pure solvents has been investigated. Narrowly sieved crystals were suspended as seeds and allowed to grow and agglomerate at constant supersaturation and temperature. Particles from each experiment were examined by image analysis and multivariate data evaluation, for the number of crystals per particle. From the resulting number distribution, parameters defining the "degree of agglomeration" were extracted. The degree of agglomeration among the product particles is fairly low in water, methanol, and ethanol, while it is substantial in acetone particularly, but also in acetonitrile and methyl ethyl ketone. Surfaces of large, well-grown paracetamol crystals have been characterized by contact angle measurements. The surface free energy components of different crystal faces have been estimated using Lifshitz–van der Waals acid–base theory. The data are used for estimation of the solid–liquid interfacial free energy of each face in the solvents of the agglomeration experiments and the corresponding crystal–crystal adhesion free energy of pairs of faces. The degree of agglomeration in different solvents does correlate to the free energies of adhesion. This supports the hypothesis that the influence of the solvent on the crystal agglomeration relates to physico-chemical adhesion forces between crystal faces in the solution. © 2007 American Institute of Chemical Engineers *AIChE J,* 53: 2590–2605, 2007

Keywords: crystal growth (industrial crystallization), surface chemistry/physics, fluid mechanics, particle technology

Introduction

In the design of a crystallization process for an organic compound, the selection of the solvent is of key importance. The solvent very much determines the solubility and the conditions for supersaturation generation, and hence the productivity and the yield of the process. The solvent also influence on the kinetics of nucleation and crystal growth, and hence on the crystal shape, crystal size distribution, and degree of agglomeration. When agglomeration is pronounced it controls the product particle size distribution and particle morphology, and hence very much determines the conditions for filtration, washing, drying, and product formulation, as well as the end-use properties like dissolution and bioavailability of pharmaceuticals.

Agglomeration in solution is in principle a three-step process: (i) crystals collide, (ii) adhere, and (iii) grow together. After collision, physico-chemical and fluid mechanical forces compete and determine the life-time of the aggregate, and hence the time available for growing the crystalline bridges within the agglomerate. All three steps of the agglomeration process are influenced by the properties of the solvent. Previous work on agglomeration has been reviewed elsewhere.[1,2]

In our earlier work, agglomeration of paracetamol in various pure solvents and solvent mixtures was investigated by

Correspondence concerning this article should be addressed to Å. C. Rasmuson at rasmuson@ket.kth.se.

crystallization experiments,[1,3] and it was found that the degree of agglomeration decreases with increasing solvent polarity. However, even though the initial supersaturation was equal and the overall mass deposition was roughly the same, the supersaturation changed significantly during each experiment and the particle size distribution was uncontrolled. In more refined fully seeded isothermal agglomeration experiments[2] operated at constant supersaturation in acetone–water mixtures it was established that the influence of the solvent composition cannot be explained by differences in crystal growth rate or differences in solution viscosity, and the results were very well correlated to the polarity of the solvent. Unfortunately, the solvent polarity is not a well-defined property and it does not provide a basis for deeper insights. However, the results suggest that the molecular crystal–solvent interactions and the physico-chemical adhesion forces between crystals are of significant importance. If the adhesion forces are strong enough the crystals are kept together for a sufficiently long time for crystal growth to establish crystalline bridging by which agglomerates are formed.

The aim of the present work is to establish whether the results on the influence of the solvent on the agglomeration of paracetamol can be explained and correlated to an independent assessment of the interfacial properties and the adhesion forces of paracetamol crystal faces in different solvents. Adhesion forces can be characterized by the thermodynamic free energy of adhesion between solid surfaces in the solution and can be calculated from the relevant solid–liquid interfacial energies. Unfortunately, solid–liquid interfacial energies cannot be easily measured.[4] In the present work we have determined the contact angle of different probe solvents on different faces of large well-grown paracetamol crystals. The data are used within the Lifsnitz–van der Waals acid–base theory of van Oss et al.[5] to estimate the surface free energy components, based on which the solid–liquid interfacial free energy of different faces is estimated.

Many adhesion phenomena, from coating on surfaces to clustering of colloidal particles and bacteria, can be explained and quantified by the free energy of adhesion, as is reviewed by Clint.[6] Bramley et al.[7] tried to describe the agglomeration of calcium oxalate in aqueous solution by application of the DVLO theory, but without success. According to van Oss[8] often the DLVO theory alone does not work in water, since acid–base forces (due to hydrogen-bonding) are often much stronger than both Lifshitz–van der Waals and electrostatic double-layer forces.

To our knowledge, the Lifshitz–van der Waals acid–base approach has not been applied previously to explain the agglomeration behavior in a crystallization process. However, the theory has been used in other studies. Clear and Nealey[9] measured the force of adhesion with atomic force microscopy between surfaces modified with self-assembled monolayers (SAMs). Measurements were made with the surfaces immersed in various solvents (hexadecane, ethanol, 1,2-propandiol, 1,3-propandiol, and water) and an excellent agreement with the free energy of adhesion calculated from surface free energy components was obtained. For hydrophobic SAMs, Kokkoli and Zukoski[10] report increased adhesion forces with increasing solvent contact angle. It demonstrates how the interaction between hydrophobic surfaces can be modified through a change in solvent composition, i.e. surface wettability. In a similar way, Muster and Prestidge[11] found that faces of *N*,*n*-octyl-D-gluconamide crystals and of two polymorphic forms of sulfathiazole, being less hydrophobic surfaces than the SAM surfaces of Kokkoli and Zukoski,[10] also exhibit an approximately linear relation between the adhesion force and the contact angle of water. Freitas and Sharma[12,13] have studied the effect of hydrophobicity on the hydrodynamic detachment of colloidal particles from surface substrates in various solvents (water, ethanol, benzene, toluene, etc.). Good qualitative agreement was obtained between the calculated free energy of adhesion (from surface free energy components) and the critical hydrodynamic force required to detach the particles, as well as measured pull-off forces. This gives support for the usefulness of the Lifshitz–van der Waals acid–base approach in estimating interfacial free energies between surfaces in liquid media. However, on the other hand, there is also controversy concerning the van Oss theory as is discussed in various papers (e.g. Refs. 14, 15).

With respect to the present study, determination of contact angles is not controversial in theory, but there are experimental problems. We examine surfaces that are not perfectly smooth since it would be difficult to grow such surfaces of paracetamol and the surfaces are not smooth in our agglomeration experiments. Furthermore, the solvents are not saturated with paracetamol so there may be some dissolution. However, saturated solutions could not be used since there are only surface energy parameter values for pure solvents. There is controversy concerning the Lifshitz–van der Waals acid–base theory of van Oss, but as far as known to us there is really no other route to follow to estimate the free energy of adhesion for the crystals that we are interested in and in the solvents of industrial relevance. However, since the theory is under debate and in our work we find values on the interfacial energy that sometimes are not realistic, the values determined are mainly of interest in a relative sense and for comparison with our agglomeration results. The main result of the work is that we do find a correlation between our agglomeration results and our estimated free energies of adhesion. Hence, even if the free energy values as such can not be fully trusted, this trend lends support to our hypothesis that the influence of the solvent on the agglomeration is due to differences in the crystal–crystal adhesion. This is of importance and encourages further studies into this area.

Theory

From wetting thermodynamics, a pure liquid droplet placed on a flat, smooth, and homogeneous solid surface takes the shape that minimizes the free energy (γ) of the system. This is described by the classical Young's equation:

$$\gamma_S - \gamma_{SL} = \gamma_L \cos\theta \tag{1}$$

Two out of four quantities in Eq. 1 are directly measurable: the contact angle (θ) formed between the liquid (L) and the surface of the solid (S), and the surface free energy of the liquid (γ_L). Then, in principal, only the difference $\gamma_S - \gamma_{SL}$

can be determined experimentally. Still γ_S and γ_{SL} are assumed to have unique values for a given solid (or crystal surface).

A combination of Eq. 1 with the Dupré equation, defining the free energy of solvation of a surface in a solution:

$$\Delta G_{SL} = \gamma_{SL} - \gamma_S - \gamma_L \tag{2}$$

leads to

$$\Delta G_{SL} = -\gamma_L(1 + \cos\theta) \tag{3}$$

called the Young–Dupré equation. An interpretation of this equation is that the shape of the liquid drop reflects the free energy of adhesion between the liquid and the solid.

To assess values of the nondirectly-measurable parameters γ_S and γ_{SL}, the Lifshitz–van der Waals acid–base theory proposed by van Oss et al.[5] is used. The Lifshitz–van der Waals acid–base theory is a semiempirical approach applied to classical wetting thermodynamics. In this approach, the total surface free energy comprises a nonpolar Lifshitz–van der Waals (LW) component and a polar Lewis acid–base (AB) component.

For liquid and solid surfaces:

$$\gamma_i = \gamma_i^{LW} + \gamma_i^{AB} = \gamma_i^{LW} + 2\sqrt{\gamma_i^+\gamma_i^-}, \quad i = S, L \tag{4}$$

where γ_i^+ and γ_i^- are defined as the nonadditive electron-accepting and electron-donating surface free energy parameters, respectively.

For the solid/liquid interface:

$$\gamma_{SL} = \gamma_{SL}^{LW} + \gamma_{SL}^{AB} \tag{5}$$

where

$$\gamma_{SL}^{LW} = \left(\sqrt{\gamma_S^{LW}} - \sqrt{\gamma_L^{LW}}\right)^2 \tag{6}$$

and

$$\gamma_{SL}^{AB} = 2\left(\sqrt{\gamma_S^+\gamma_S^-} + \sqrt{\gamma_L^+\gamma_L^-} - \sqrt{\gamma_S^+\gamma_L^-} - \sqrt{\gamma_S^-\gamma_L^+}\right) \tag{7}$$

Using Eqs. 2–7, the Young–Dupré equation can be rewritten as

$$(1 + \cos\theta)\gamma_L = 2\left(\sqrt{\gamma_S^{LW}\gamma_L^{LW}} + \sqrt{\gamma_S^+\gamma_L^-} + \sqrt{\gamma_S^-\gamma_L^+}\right) \tag{8}$$

In Eq. 8 there are three surface free energy parameters for the solid (γ_S^{LW}, γ_S^+, γ_S^-) and there are four surface free energy parameters for the liquid (γ_L, γ_L^{LW}, γ_L^+, γ_L^-). For certain liquids the four parameters have been determined and can be found in the literature.[8] By measuring the contact angle for each of three probe liquids (with known γ_L, γ_L^{LW}, γ_L^+, γ_L^-) on the same solid surface, three equations are obtained by which the three unknowns: γ_S^{LW}, γ_S^+, γ_S^- can be estimated. Finally, Eq. 4 and Eqs. 5–7 allow for calculation of γ_S and γ_{SL}.

The free energy of adhesion between two solid surfaces (S_1 and S_2) immersed in a liquid (L) can be calculated following Dupré (Eq. 2):

$$\Delta G_{S_1LS_2} = \gamma_{S_1S_2} - \gamma_{S_1L} - \gamma_{S_2L} \tag{9}$$

The free energy of adhesion between two surfaces of the same chemistry ($S_1 = S_2 = S$, $\gamma_{SS} = 0$) immersed in a liquid (L) is then expressed by

$$\Delta G_{SLS} = -2\gamma_{SL} \tag{10}$$

A positive value of the free energy of adhesion denotes repulsion between the particles, whereas a negative value signifies attraction.

Determination of surface free energies using the Lifshitz–van der Waals acid–base approach is controversial and the theory has been questioned.[14,15] However the theory has also been defended for its usefulness when being properly used.[16] The main controversy seems to be the determination and interpretation of the acid–base parameters (γ^+ and γ^-). The general opinion is that the negative component is too large compared to the positive component. In addition, it cannot be safely assumed that the characterisation of the solid surface is independent of the selection of the probe liquids.[17–19] Lee[20] derived a set of solvent data with more acidic parameters (more positive polar contributions) than the set of van Oss.[8] He also accounted for the equilibrium spreading pressure even though van Oss[21] asserts that this can be neglected when the surface free energy of the probe liquid is larger than that of the solid surface ($\gamma_L > \gamma_S$). Lee[20] then found that a clean and vapor adsorption free Polyvinylchloride surface is acidic while it appears to be basic based on the acid–base components of van Oss.[8] Still today there seems to be no reliable complete set of parameters.[16] The results obtained with the theory depend on the selection of probe liquids and the corresponding parameters, and are valuable mainly for a relative comparison. It is very important to select probe liquids representing dispersive, acidic and basic conditions to have a well-conditioned problem. In the present work, water, formamide, and diiodomethane are used as being considered to be a good set.[16]

Experimental

Experiments have been performed in which seed crystals were allowed to grow and agglomerate in agitated vessel experiments at constant supersaturation, crystal size, and crystal number concentration. In addition, large single crystals have been grown and different faces have been characterized by contact angle measurements. Paracetamol of pharmaceutical grade (donated by AstraZeneca, Södertälje, Sweden) and proanalysis solvents: methanol (>99.8%, BDH), ethanol (<99.7%, Primalco), acetone (>99.5%, Merck), methyl ethyl ketone (>99.5%, Merck), acetonitrile (>99.5%, Merck), ethyl acetate (>99.5%, Merck) were used. The water was distilled and filtered (0.2 μm) prior to use.

Crystallization experiments

Seeded, isothermal crystallization experiments were performed at 16°C in supersaturated solutions of paracetamol in different pure solvents: water, ethanol, methanol, acetone, methyl ethyl ketone, ethyl acetate, and acetonitrile. The experiments were performed in a 150-ml (6 cm in diameter) jacketed crystallizer with baffles and a three-blade propeller

Figure 1. Seeds (90–125 μm).

(2.5 cm in diameter) operating at 400 rpm. About 0.1 g of narrowly sieved seeds (sieve size fraction: 90–125 μm) were added to the supersaturated solution. The seeds are shown in Figure 1. The seeds were allowed to grow and agglomerate for 4 min or for 60 min. For a crystallization time of 4 min the supersaturation decay was less than 10%, i.e. the supersaturation is almost constant. A few experiments were conducted for 60 min, but in this case the supersaturation decay was significant. The production of seed crystals, experimental set up, and detailed procedures of the crystallization experiments are described elsewhere.[2] The experimental conditions are summarized in Table 1.

Production of large single crystals

Large (5 mm $\times$ 10 mm $\times$ 10 mm) single crystals were produced from an ethanol solution by very slow cooling ($\sim$0.1°C/day) crystallization. A paracetamol-saturated ethanol solution was prepared at 25°C. The solution was filtered and poured into a 500-ml jacketed crystallizer (10 cm in diameter) with a three-blade propeller (2.5 cm in diameter). Flawless seed crystals (1 mm $\times$ 1 mm $\times$ 1 mm) were carefully chosen among crystals grown by solvent evaporation from a paracetamol saturated ethanol solution at room temperature, and were placed well separated from each other at the bottom of the reactor. The temperature in the reactor was kept at 25°C overnight. The crystals were then allowed to grow by lowering the temperature manually by 0.1°C/day. The agitation rate was 150 rpm. After about a week, the crystals were filtered and rinsed with distilled water. A new saturated solution was prepared and the slow cooling crystallization was repeated for the same crystals. This procedure was repeated until the crystals reached the desired size. At the end, the crystals were carefully removed from the reactor, rinsed with distilled water, and stored in boxes.

Contact angle measurements

The sessile drop method was employed for characterization of surface free energies on large single crystals. Equilibrium contact angles of pure water (ultra high quality from a Milli-Q system), diiodomethane (>99%, Aldrich), and formamide (>99.5, BDH) drops ($\approx$1 μl) on different faces of the paracetamol crystals were determined with a goniometer (A-100, Ramé Hart) attached to a microscope. Before the contact angle measurements, the crystal surfaces were rinsed with distilled water and dried with pressurized nitrogen. Each drop was placed on a fresh spot on the crystal surface. The contact angle was then measured on two sides of each drop. The difference between the two contact angle measurements on the same drop was at most 5°. Measurements were made on six crystals and four different faces of each crystal: {001}, {110}, {20$\bar{1}$}, and {011}. At least two drops of each liquid was placed on each crystallographic face. Probe liquids with relatively low paracetamol solubility were selected to avoid strong dissolution and thereby destruction of the crystal face. However, after the measurements using

Table 1. Experimental Conditions in Seeded Crystallization Experiments

Solvent	Polarity*	Solubility,† g/kg	ln$S$‡	Impeller Re§	Kolmogorv Microscale,¶ μm	Crystallization Time, min	Mass Deposition,** g
Water	1.000	17.4	0.3	4.2×10^3	107	4	0.16
			0.2			4	0.06
MeOH	0.762	371.6	0.2	5.4×10^3	88	4	0.40
			0.1			4	0.07
			0.05			60	0.07
EtOH	0.654	232.8	0.2	2.8×10^3	146	4	0.04
AcN	0.460	32.8	0.2	9.1×10^3	59	4	0.15
AcO	0.355	111.6	0.2	11.1×10^3	51	4	0.05
			0.1			4	–
			0.1			60	0.12
MEK	0.327	70.0	0.2	8.4×10^3	63	4	0.07
EtAc	0.228	10.7	0.4	8.2×10^3	64	4	0.11
			0.2			4	0.03
			0.2			60	0.19

*Normalized E_T-values.[22]
†Solubility of paracetamol at 30°C.[23]
‡Supersaturation S is defined as the ratio of the solute concentration to the solubility concentration at 16°C.
§$Re = \frac{ND^2}{\nu}$.
¶$\lambda_K = \left(\frac{\nu^3}{\bar{\varepsilon}}\right)^{0.25}$, $\bar{\varepsilon} = \frac{N_p N^3 D^5}{V}$, $N_p = 0.4$.[24]
**Calculated from solution concentrations before and after crystallization, determined gravimetrically by evaporating samples to dryness.

drops of water and formamide, dissolution spots or rings were observed on the faces.

Single-crystal X-ray diffraction

A small piece of crystal (1 mm × 1 mm × 1mm), cut from each crystal after the contact angle measurements, was mounted and held by grease on a capillary. The capillary-mounted crystal was indexed by optical goniometry and X-ray single crystal diffractometry to give Miller indices for the faces of the large crystal with respect to the monoclinic space group symmetry $P2_1/n$ (the unit cell parameters: a = 7.0939 Å, b = 9.2625 Å, c = 11.6570 Å, and β = 97.6720°).[25] In this paper the faces are matrix transformed and named in the space group symmetry $P2_1/a$ since it is normally used in the literature for paracetamol crystals.

Methods of Evaluation

Product particle characterization

Particles from the seeded crystallization experiments in pure solvents were examined under a microscope to determine the degree of agglomeration. First, image analysis was used to measure image descriptors of about 300 particles from each crystallization experiment. The image descriptor data were then processed by principal component analysis (PCA) together with the corresponding data of a set of selected calibration particles. The processing is such that the PCA loading-plot is determined by the calibration particles, and hence becomes equal for all samples. Accordingly, the score position of a sample particle characterizes the particle in a fixed principal component frame. The number of crystals in each particle of the calibration set was counted manually in order to construct a correlation between the C/A number (number of crystals per agglomerate) and the principal component score position. This correlation was then used to estimate the C/A number of a sample particle from its principal component score position value. A C/A number equal to unity means that the particle is a single crystal. Increasing C/A-numbers denote larger numbers of crystals grown together in the particle (agglomerate). The number fraction of the particles in a sample having a C/A number less than 2 is used as a measure of the degree of agglomeration. An increasing number fraction corresponds to a decreasing degree of agglomeration. Details of descriptor selection, use of PCA, and the calibration model have been presented earlier.[1,3]

Surface free energy parameters and free energy of adhesion

The surface free energy parameters (γ_S^{LW}, γ_S^+, γ_S^-) of each face were calculated using the surface free energy parameters of the probe solvents (Table 2) and the measured contact angles (Table 3) in Eq. 8. For each face and each probe liquid the contact angle was determined several times. Instead of averaging the contact angle value for each face and probe liquid before solving for the three unknowns of Eq. 8, all individual measurements were supplied into a direct optimization using the Gauss–Newton method as implemented in the MATLAB optimization toolbox. The three unknown surface free energy components of each face were determined such that the sum of the least squares deviation between measured and calculated contact angles was minimized. Knowing the surface free energy parameters (γ^{LW}, γ^+, γ^-) for the crystal surfaces and the solvents used in the crystallization experiments (Table 4), each respective interfacial free energy γ_{SL} can be calculated from Eqs. 5–7. By Eqs. 9 and 10 the free energy of adhesion between different faces depending on the solvent can be calculated.

Table 2. Polarity[22] and Surface Free Energy Parameters[8] (mJ/m^2) of Probe Liquids

Liquid	Polarity	γ_L^{LW}	γ_L^+	γ_L^-	γ_L^{AB}	γ_L
Water	1.000	21.8	25.5	25.5	51.0	72.8
Diiodomethane	0.179	50.8	0	0	0	50.8
Formamide	0.799	39.0	2.28	39.6	19.0	58.0

Table 3. Contact Angles of the Four Examined Crystal Faces

Crystal Face	θ,* degree			
	Pure Water	Water (PA Sat.)	CH_2I_2	Formamide
{001}	21 ± 2 (3)	22 ± 1 (3)	41 ± 3 (3)	10 ± 2 (3)
{110}	53 ± 3 (9)	62 ± 5 (4)	40 ± 4 (7)	33 ± 5 (5)
{20$\bar{1}$}	37 ± 1 (3)	39 (1)	33 ± 2 (3)	19 ± 3 (3)
{011}	42 ± 3 (3)	46 ± 3 (3)	37 ± 6 (4)	10 ± 2 (2)

*Mean values, and standard deviations for the number of drops given in parentheses.

Molecular modeling of crystal faces

The program Mercury 1.2.1 (2004) (a free download program from the Cambridge Crystallographic Data Center) was used to visualize the crystal structure and explore the molecular arrangement at the different crystal faces of the monoclinic form of paracetamol. Crystallographic data in the space group symmetry $P2_1/n$ (the unit cell parameters: a = 7.0939 Å, b = 9.2625 Å, c = 11.6570 Å, and β = 97.6720°) by Naumov et al.[25] was adopted. A packing and slicing tool of the program was used to place a plane (named by its Miller indices) through the crystal lattice. In this way the molecular orientation at the selected place could be examined. Noteworthy, in this paper, the planes are matrix transformed and named in the space group symmetry $P2_1/a$. Functional groups of particular interest are the hydroxyl (—OH) group and the amide (—NHC=O—) group of the paracetamol molecule. Both these groups can act as both H-bond acceptor and

Table 4. Polarity[22] and Surface Free Energy Parameters[8] (mJ/m^2) of Liquids

Liquid	Polarity	γ_L^{LW}	γ_L^+	γ_L^-	γ_L^{AB}	γ_L
Water*	1.000	21.8	25.5	25.5	51.0	72.8
Methanol*	0.762	18.2	0.06	77	4.3	22.5
Ethanol*	0.654	18.8	0.02	68	2.6	21.4
n-Octanol	0.537	27.5	0	18.0	0	27.5
Dimethylsulfoxide	0.444	36.0	0.5	32.0	8.0	44.0
Methyl ethyl ketone*	0.327	24.6	0	24.0	0	24.6
Ethyl acetate*	0.228	23.9	0	19.2	0	23.9
Tetrahydrofuran	0.207	27.4	0	15.0	0	27.4
Toluene	0.099	28.5	0	2.3	0	28.5

*Solvents used in crystallization experiments.

H-bond donor. The four faces examined for contact angle data were explored.

Results

Agglomeration in crystallization experiments

Microscopy images of particles after 4-min crystallization in four pure solvents are given in Figure 2. In water and acetonitrile the crystal habit is very little changed from the flat and tabular habit of the seed crystals (Figure 1). This is also true for crystals grown in ethanol, methyl ethyl ketone and acetone (not shown). Crystals grown in methanol and ethyl acetate appear to be somewhat different with a more rhombic and columnar habit, respectively. However, the main characteristic difference between the particles from crystallization in different solvents is related to the degree of agglomeration. The cumulative C/A-number distributions are given in Figure 3 quantifying the agglomeration behavior of the product particles. In all these experiments the supersaturation was $\ln S = 0.2$, and the time for growth and agglomeration was 4 min. The agglomeration is quite pronounced in acetone, methyl ethyl ketone, and acetonitrile, but less significant in water, the alcohols, and ethyl acetate. The $(C/A)_{50}$-values in water, methanol, ethanol, and ethyl acetate range from 1.8 to 2, i.e. not far from the value for the seeds: 1.5. In acetonitrile and in methyl ethyl ketone the $(C/A)_{50}$-values increase to 2.4 and 2.7, respectively, and in acetone to 3.8. The C/A-distributions tend to become broader as the $(C/A)_{50}$-value increases. In acetone, there is obviously a quite wide range of properties among the product particles. These results are in good agreement with visual microscopic observation of the particles.

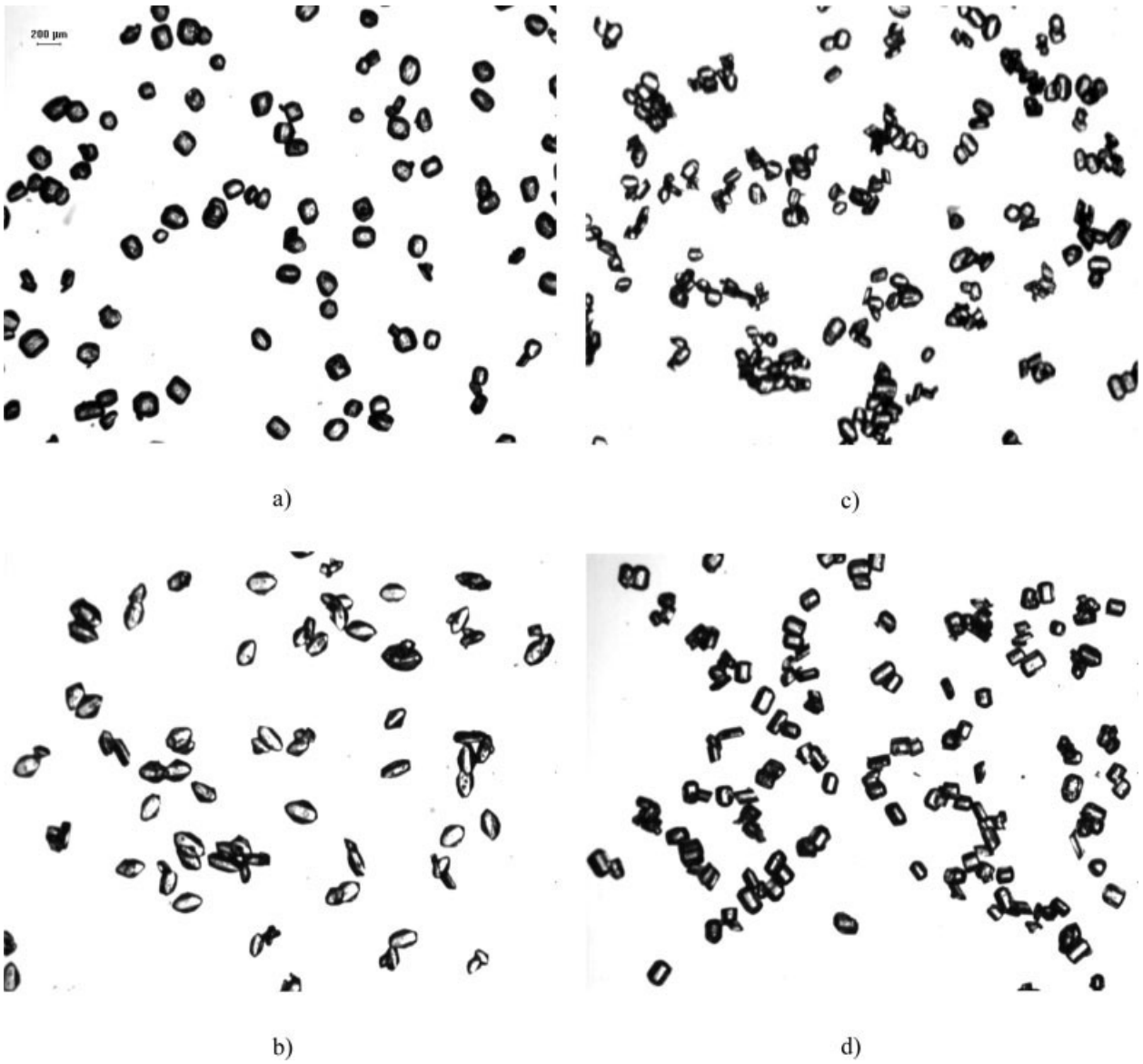

Figure 2. Particles after 4-min crystallization in: (a) water ($\ln S = 0.2$), (b) methanol ($\ln S = 0.2$), (c) acetonitrile ($\ln S = 0.2$), and (d) ethyl acetate ($\ln S = 0.4$).

All pictures are captured at same magnification.

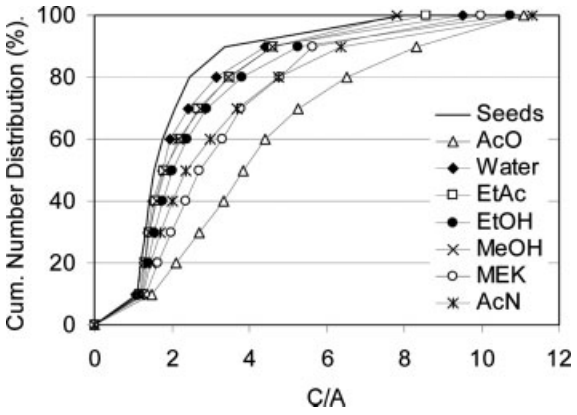

Figure 3. C/A-number distributions of seeds and formed particles after 4-min crystallization in acetone, water, ethyl acetate, ethanol, methanol, methyl ethyl ketone, and acetonitrile (ln$S$ = 0.2).

The influence of crystallization time as well as of supersaturation on the agglomeration is shown in Figure 4 for ethyl acetate, acetone, and methanol. Obviously, an increased time allows for further agglomeration. At constant supersaturation (ln$S$ = 0.2) in ethyl acetate the $(C/A)_{50}$-value increases from 1.8 to 4.5, when the time is extended from 4 to 60 min. In acetone, at a supersaturation of ln$S$ = 0.1, the $(C/A)_{50}$-value increases from 3.4 to 5.9, and in methanol it increases from 1.8 at ln$S$ = 0.1 to 2.8 at ln$S$ = 0.05 when the time is extended from 4 to 60 min. Figure 4 reveal that a higher supersaturation leads to a higher degree of agglomeration in ethyl acetate, while the influence of supersaturation is quite weak in acetone and insignificant in methanol.

Characterization of crystal surfaces

The probe liquid contact angles (mean value ± SD) on four faces of the paracetamol crystal are given in Table 4. A low contact angle denotes a low solid–liquid interfacial energy, i.e. a high affinity of the solvent to the surface. The contact angles of water reveal that {001} is the most hydrophilic face. The $\{20\bar{1}\}$ and {011} faces are less hydrophilic than {001}, while the {110}-face is the least hydrophilic of all four faces. Diiodomethane is the least polar solvent (E_T = 0.179) and has the lowest surface tension to air of the probe liquids used (Table 2). The contact angle of diiodomethane is around 40° for all faces, suggesting that none of the surfaces is particularly nonpolar. Formamide has a high Reichardt polarity index value (E_T =0.799), but it is lower than for water (E_T =1.000). The contact angles of formamide are substantially lower than those of pure water. Both formamide and water have their lowest affinity to the {110}-face. The contact angle of an aqueous solution saturated by paracetamol is consistently somewhat larger than that of pure water on the {001}, $\{20\bar{1}\}$, and {011} faces, while it is significantly larger on the {110}-face.

Table 5 presents the calculated surface free energy parameters of the four faces. The surface free energy ranges from 50 to 57 mJ/m^2. On all faces the Lifshitz–van der Waals contribution γ_S^{LW} is in the range of 40 mJ/m^2 and it is 2–4 times higher than the acid–base contribution γ_S^{AB}. All the faces show a strong negative polar component γ_S^- to the surface free energy. The largest difference between the faces is found in this negative polar component. The negative polar component of the {001}-face is significantly stronger than that of the other faces. The contact angle of pure water is well correlated to the inverse of the value of the negative po-

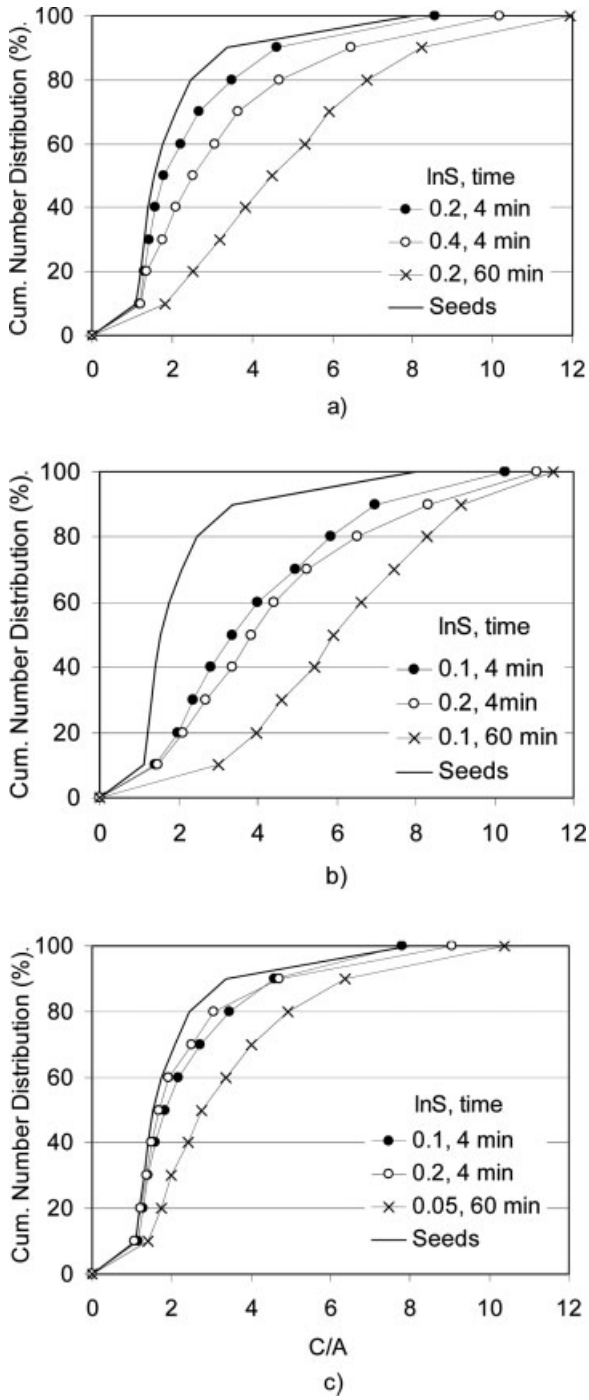

Figure 4. C/A-number distributions of seeds and formed particles after crystallization at different experimental conditions in: (a) ethyl acetate, (b) acetone, and (c) methanol.

Table 5. Calculated Surface Free Energy Parameters (mJ/m^2) with Standard Deviation of the Four Examined Crystal Faces

Crystal Face	γ_S^{LW}	γ_S^+	γ_S^-	γ_S^{AB}	γ_S
{001}	38.9 ± 0.5	1.7 ± 0.1	47.5 ± 0.8	18.0 ± 1.1	56.9 ± 1.2
{110}	39.7 ± 0.5	1.2 ± 0.2	21.8 ± 1.3	10.2 ± 1.8	49.9 ± 1.9
{20$\bar{1}$}	43.1 ± 0.4	1.1 ± 0.1	33.8 ± 1.1	12.2 ± 1.2	55.3 ± 1.2
{011}	41.0 ± 0.8	2.5 ± 0.3	26.3 ± 2.2	16.2 ± 2.4	57.2 ± 2.5

lar component, and the contact angle of diiodomethane is well correlated to the inverse of the value of the Lifshitz–van der Waals component.

Molecular arrangements at the four examined faces are shown in Figure 5. The surfaces are characterized by polar groups—hydroxyl and acetamide—that can act as H-bond acceptors as well as donor. The surfaces are also characterized by aromatic rings with π-electrons that can act as weak H-bond acceptors. According to Figure 5, the paracetamol molecules at the {001} face are stacked so that hydroxyl and amide groups are exposed at the surface, at the same time as all the aromatic rings are somewhat exposed. All the other three faces also expose H-bonding sites, but at the same time the π-electrons of the aromatic rings are more buried inside the surfaces. On the {20$\bar{1}$}-face all the aromatic rings are stacked perpendicular to the face.

Solid–liquid interfacial free energy

The solid–liquid interfacial free energy is by definition the thermodynamic free energy change required in forming a unit of new interface between the solid and the liquid, and it is a parameter strongly related to the crystal–solvent interaction. If the affinity of the solvent to the crystalline surface is high the interfacial free energy is low. The calculated solid–liquid interfacial free energy values for the solvents used in the crystallization experiments are given in Table 6. Unfortunately, there are no parameter values in the literature for the free energy components of acetone and acetonitrile. The calculated values of Table 6 range from -11.3 to $+8.4$ mJ/m^2. All values are positive in methyl ethyl ketone and in ethyl acetate, while negative values are found in water, methanol, and ethanol. The overall numerical magnitude is in accordance with data of other organic compounds,[26] but as discussed later, for this experimental system negative values do not fit into the classical thermodynamic theory of crystal nucleation.

Free energy of adhesion

Depending on how the different faces of the crystals are paired together, there are 10 different free energies of adhesion in each solvent. In four of these cases the two surfaces are crystallographic equal and in the present study assumed equal in their surface free energies. Then Eq. 10 can be used. For the other six cases Eq. 9 is used. The results are presented in Figure 6. A positive value of the adhesion free energy suggests repulsion between the surfaces, while a negative value signifies attraction. As shown in Figure 6, in methanol and ethanol the adhesion free energy of different combinations of crystal surfaces is mostly positive (repulsive), while in methyl ethyl ketone and ethyl acetate the situation is opposite with only negative (attractive) values of the free energy of adhesion. The result in water is more complex, as all calculated adhesion free energies where the {001}-face is involved are strongly positive (repulsive), while most of the other combinations lead to negative (attractive) free energy values.

Evaluation and Discussion

Contact angle measurements

The contact angle theory based on Young's equation (Eq. 1) assumes an ideal solid surface that is flat, smooth, chemically homogeneous, insoluble, etc. On rough surfaces, the apparent contact angle may be different from the ideal contact angle of Young's equation. Muster and Prestidge[11] relate a lower contact angle of water to greater coverage of hydrophilic groups of the crystal surface, but they also point out that a larger contact angle on a specific crystal surface coincides with a higher growth rate and higher surface roughness. Indeed, the determined contact angle of water on the four studied faces of the present work increases and follows the same order as the specific surface growth rate (data of Ristic et al.[27]). This possibly means that the observed increased contact angle in the order: {001}, {20$\bar{1}$}, {001}, and {110} also relates to surface roughness and not only to surface chemistry. Figure 7 shows SEM images of a large crystal never used for contact angle measurements. As expected, the crystal surfaces exhibit a microscopic roughness. A closer look at the edge between two faces (Figure 7b, point b in Figure 7a) reveals the occurrence of short and pronounced growth steps. More long and regularly spread growth steps are observed all over the crystal faces, and in particular on the {011}-face (Figure 7a). An increased magnification shows that the growth steps and other defects also exist on the {110}- and {001}-faces (Figures 7c, d, respectively). However, in our contact angle measurements the drops are sufficiently large compared in the scale of the face roughness, and the spreading of the liquid drops is observed to be axisymmetric, i.e. the three-phase contact line is circular. Furthermore, the increased contact angle with surface roughness, as observed by Muster and Prestidge[11] and in the present work, is opposed to the established Wenzel's theory. According to Wenzel's theory[28] an increased roughness allows for a larger actual solid–liquid interface than the geometric droplet area and thus the apparent contact angle decreases with increasing roughness (if the ideal contact angle is smaller than 90°). Hence, the roughness of the crystal surfaces is not considered to be a significant obstruction in the measurements and the observed increased contact angle of water in the order: {001}, {20$\bar{1}$}, {001}, and {110} relates almost certainly to the surface chemistry.

A problem likely to be more important is the destruction of the surface due to dissolution into the unsaturated liquid droplet. However, since surface free energy parameters are only available for pure liquids, we could not have used liquids saturated by paracetamol for the surface energy deter-

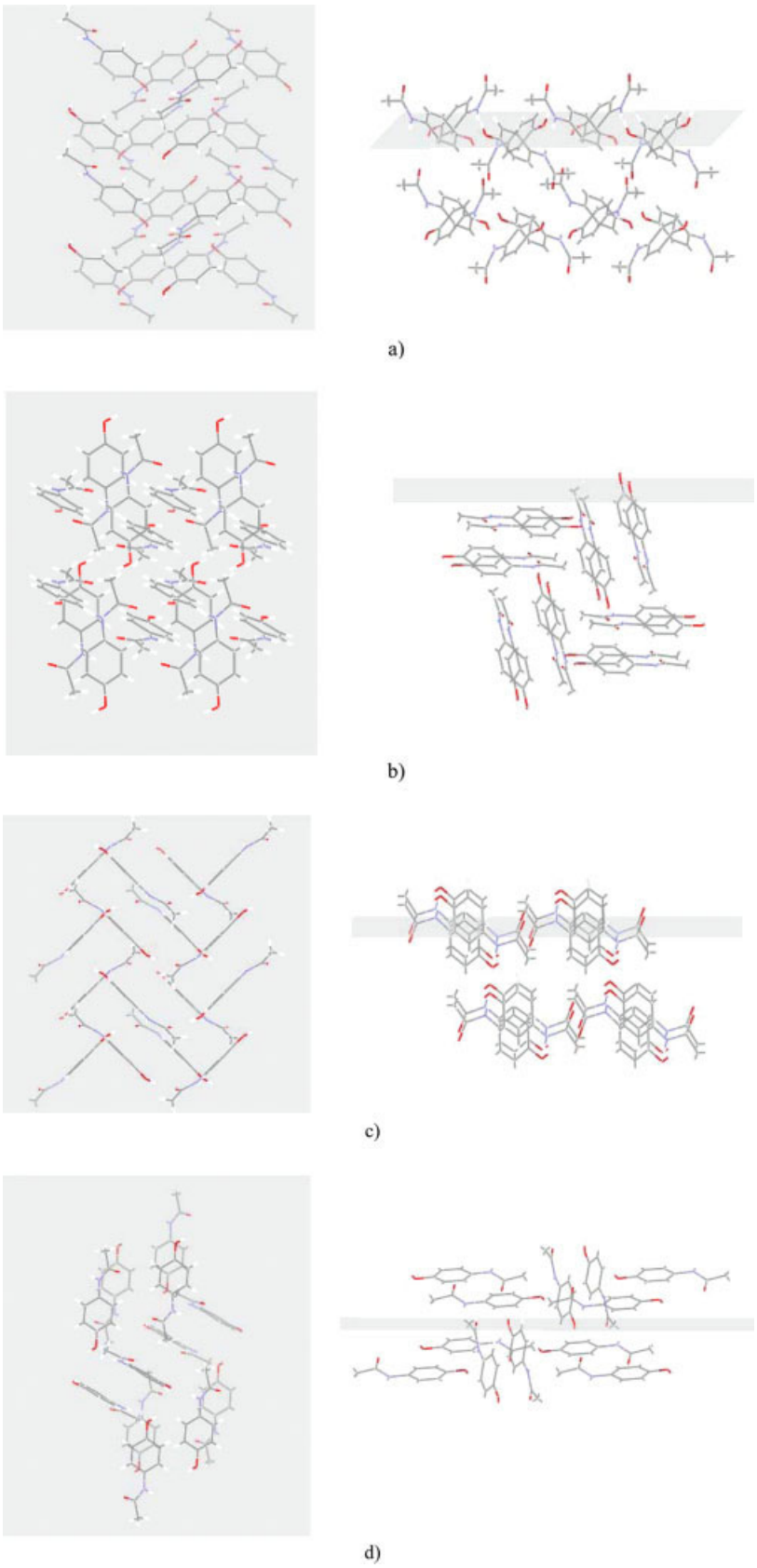

Figure 5. Molecular arrangement at different crystal face planes: (a) {001}, (b) {110}, (c) {20$\bar{1}$}, and (d) {011}.
Left: perpendicular direction to the plane.

Table 6. Calculated Solid–Liquid Interfacial Energy (mJ/m^2) for Different Solvents and Crystal Faces with Surface Free Energy Parameters According to Tables 4 and 5, Respectively

Crystal Face	Water	MeOH	EtOH	MEK	EtAc
{001}	−11.3	−0.1	0.5	6.8	8.4
{110}	4.9	−1.9	−2.1	1.6	2.8
{20$\bar{1}$}	−2.5	0.5	0.6	4.6	5.8
{011}	2.5	−5.2	−4.7	2.8	4.7

mination. As presented in Table 3, the contact angle of an aqueous solution saturated by paracetamol compared to that of pure water seems to be somewhat higher for the {001}, {20$\bar{1}$}, and {011} faces, but significantly higher only for the {110}-face. However, the contact angles of pure water and that of a saturated solution (i.e. without dissolution of paracetamol) follow at least the same trend for the different faces. This supports the hypothesis that the observed differences in the contact angle of pure water relate to the differences in surface chemistry of different faces.

Surface and interfacial free energies

For all characterized crystal faces the basic component of the surface free energy is much larger than the acidic component (Table 5), and for some faces the value of the interfacial energy is negative.

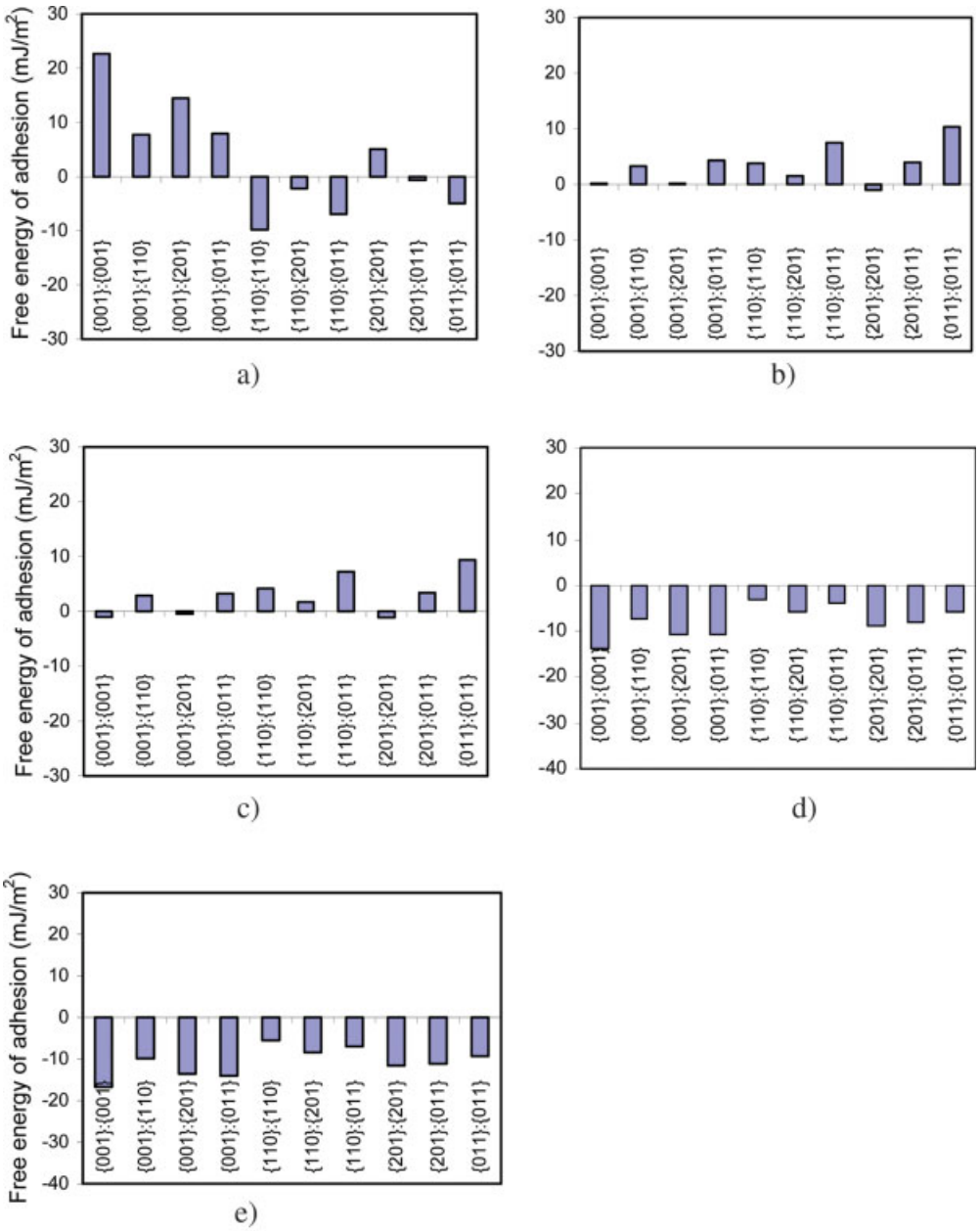

Figure 6. Free energy of adhesion of 10 different combinations of crystal surface pairs in different solvents: (a) water, (b) methanol, (c) ethanol, (d) methyl ethyl ketone, and (e) ethyl acetate.

[Color figure can be viewed in the online issue, which is available at www.interscience.wiley.com.]

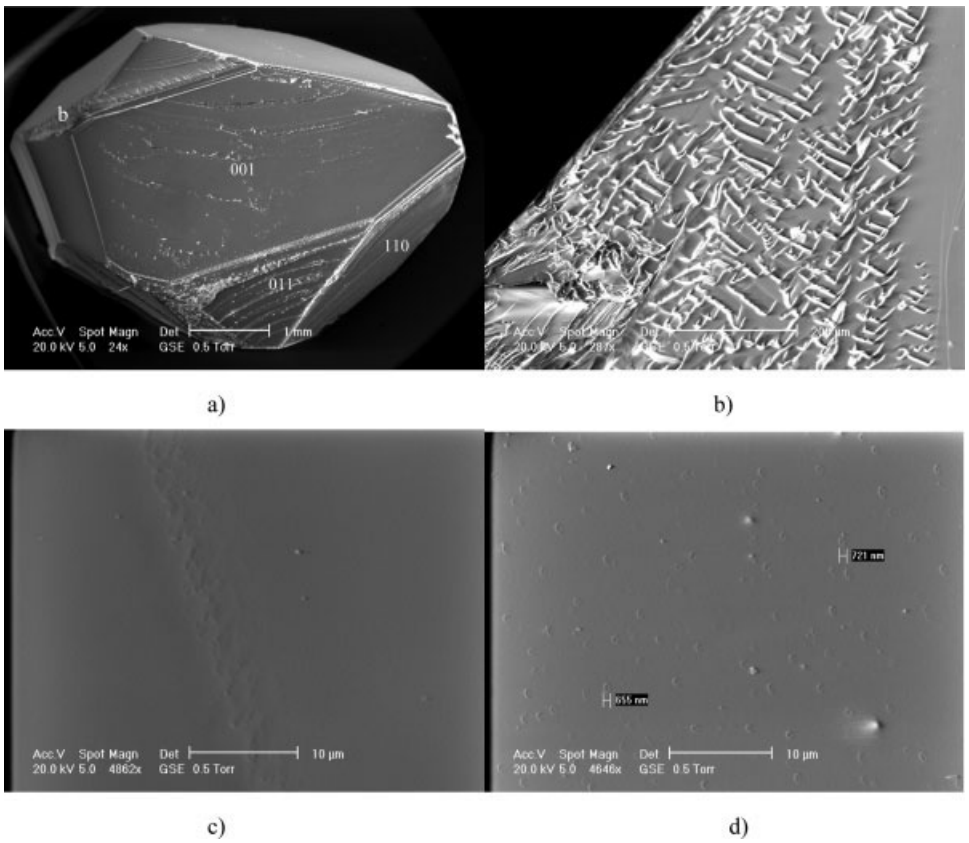

Figure 7. SEM images of (a) one large grown paracetamol crystal, (b) the edge between two faces, (c) {110}, and (d) {001}.

The calculated surface free energy components of the solid are dependent on the surface free energy components of the probe liquids which are taken from the literature. As can be seen in Table 2, the values of formamide are quite asymmetric with a pronounced role of the basic function, and for all the organic solvents in the agglomeration work (Table 4) the basic component is much larger than the acidic component. For water the negative and the positive acid–base components are balanced. To note, the values for water have not been determined by experiments but has been balanced based on theoretical arguments, and then these water values serve as a reference for all other values.

In a calculation of the electrostatic surface potential of the paracetamol molecule it is shown that the electrostatic potential varies from very positive to strongly negative and the molecule is a multipole, but without a clear dominance for electronegativity in any of the major directions.[29] The hydroxyl group has one positive hydrogen and an oxygen with two free electron pairs. The acetamide group has one positive hydrogen, a nitrogen that has one free electron pair, and in addition a carbonyl oxygen with two free electron pairs. Also the π-electrons of the aromatic ring can contribute to a more negative polar component. Hence, with respect to the molecular arrangement at the four faces in Figure 5, we expect to find a difference in the electrostatic potential among the faces. A stronger negative polar component of the {001} face could relate to that the carbonyl groups and the aromatic rings are more exposed than in the other faces. Still, it seems unlikely that the negative polar component should be very much stronger than the positive polar component. However, the molecules at the surface do not necessarily possess the same configuration as the molecules in the lattice. In particular, the orientation of the tail groups sticking out of the surface can be different. In addition, the tail groups are expected to interact and orientate differently with different solvent molecules at the surface.

Negative interfacial free energy values occur when the polar AB term of Eq. 5 is negative and its absolute value is larger than that of the nonpolar LW term. For all five solvents used in the crystallization experiments, γ_L^{LW} (Table 4) is about half the value of γ_S^{LW} (Table 5) and the $\left(\sqrt{\gamma_S^{LW}}-\sqrt{\gamma_L^{LW}}\right)^2$-term is in the order of 4. In water, the negative values of the interfacial free energy on the $\{001\}$ and the $\{20\bar{1}\}$ faces are due to the quite large $\sqrt{\gamma_S^-\gamma_L^+}$-term in Eq. 7. In a similar way, the negative values for methanol and ethanol can be analyzed and we may note that these solvents have very high values on the basic component γ_L^-. In fact, for the solid surfaces of Table 5 and for all the solvents of Table 4 except water, the basic component is much larger than the acidic component.

Negative solid–liquid interfacial free energy values are well established and accepted in contact angle and wetting studies.[21] The interfacial free energy can be negative when the adhesive forces across the interface are greater than the cohesive forces within each phase, i.e. when the solute molecules prefer to associate with the solvent instead of associating with each other. However, when the interfacial free

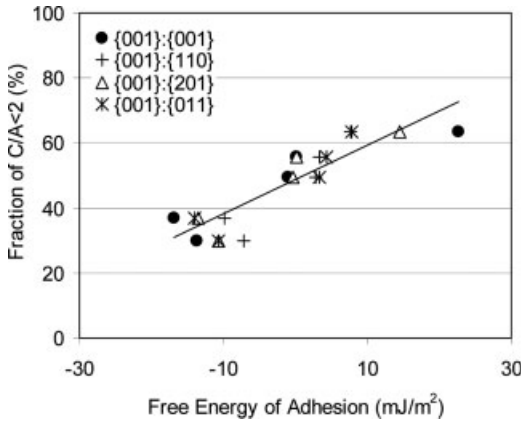

Figure 8. Change in degree of agglomeration with calculated free energy of adhesion in different solvents: water (63.3%), MeOH (55.7%), EtOH (49.3%), EtAc (37.0%), and MEK (30.0%).

Seeded crystallization experiments (4 min).

energy is negative the classical crystal nucleation theory breaks down, because the interface in that case has a lower free energy than the bulk crystal. There is no barrier for nucleation since creating the interface is thermodynamically favorable, instead of the opposite. In our previous work on nucleation[26] and growth[30] of paracetamol, no peculiarities have been observed. Furthermore, as pointed out by van Oss,[21] in a solvent where the overall interfacial free energy is negative we expect to find a very high solubility. For paracetamol in the solvents of the present work, the solubility is not exceedingly high (see Table 1). Considering the above discussion, we have reason to believe that in the present work the domination of the negative polar is exaggerated, and that in reality the interfacial free energy is never negative. Hence, values should be considered relative to one another rather than in an absolute sense. Moreover, a low degree of agglomeration is due to the attractive adhesion forces being too weak rather than actual repulsion, as suggested by a positive free energy of adhesion. When the attraction is too weak, the hydrodynamic forces can easily keep the crystals apart, thus reducing agglomeration. For example, in the case of methanol, even though the agglomeration is very low after 4 min, there is a significant agglomeration after 60-min crystallization (Figure 4c). This supports that the forces between crystals in paracetamol solutions of methanol are weakly attractive, instead of being repulsive as suggested by the adhesion free energy calculations (Figure 6b).

Agglomeration and physico-chemical conditions

The experimental results show that after 4-min crystallization there is essentially no agglomeration in methanol and ethanol, while the agglomeration is significant in methyl ethyl ketone (see Figure 3). In the alcohols the calculated adhesion free energy is positive and in methyl ethyl ketone it is negative. Hence, in a relative comparison, the calculated adhesion free energies of different combinations of crystal surfaces in these solvents (Figure 6) support the agglomeration behavior observed. According to the calculated free energy of adhesion a significant agglomeration would also be expected in ethyl acetate. However, this is not observed after 4-min crystallization. In this experiment the mass deposition is only 0.03 g ($\ln S = 0.2$, see Table 1). At very low deposition there is insufficient formation of crystalline bridges. The agglomerates will then be weak and may partly be disrupted during the filtration, washing, and characterization of the particles, and the measured degree of agglomeration will not properly reflect the conditions in the crystallizer. After 60-min crystallization a significant agglomeration is observed for seeds grown in ethyl acetate (see Figure 4a). Also a significant agglomeration is found in ethyl acetate at higher supersaturation ($\ln S = 0.4$) and 4-min crystallization. In this case the mass deposition is 0.11 g. In pure acetone and pure methanol (Figures 4b, c, respectively) as well as in the previously studied acetone–water system,[2] no significant influence of supersaturation (growth rate) on the agglomeration behavior has been observed. This supports that the ethyl acetate experiment over 4 min at low supersaturation deviates from the trend because of insufficient crystal growth mass deposition, rather than lack of sufficient attractive free energy of adhesion.

In the present evaluation, the fraction of particles in a sample having a C/A-number less than 2 is taken to be a measure of the fraction of nonagglomerated crystals. This parameter is extracted from the C/A-number distribution for a sample. A small fraction of C/A < 2 means a high degree of agglomeration, i.e. there are very few crystals that are not engaged in agglomerates. Figure 8 shows the number fraction of nonagglomerated crystals (C/A < 2) versus the calculated free energy of adhesion for the solvents (Figure 6). Because the added seeds in all experiments are flat and tabular with large grown {001}-faces, and larger faces are more likely to collide, only the combinations where at least one of two faces is a {001}-face are considered in Figure 8. As can be seen, the fraction of nonagglomerated particles increases along the free energy scale (the x-axis). If all possible face combinations are included, the overall appearance of the correlation remains the same, even though the spread is large for water.

The adhesion free energy calculations are based on the surface free energy components of pure solvents, ignoring the fact that the real agglomeration process takes place in supersaturated solutions. The surface free energy of a saturated paracetamol solution γ_L^* (68.5 mJ/m^2, Granberg[31]) does

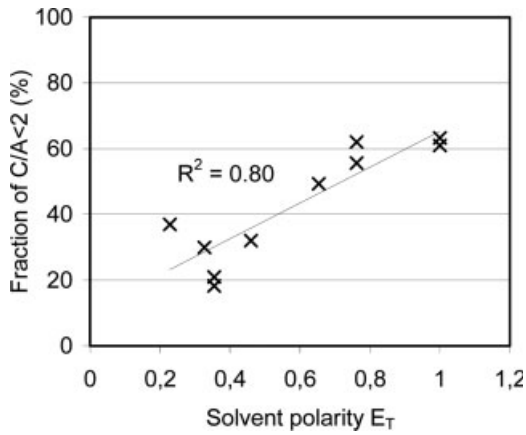

Figure 9. Change in degree of agglomeration with solvent polarity.

Solvent polarities are taken from Reichardt.[22] Seeded crystallization experiments (4 min).

not differ greatly from the surface free energy of pure water γ_L (72.8 mJ/m^2, Table 4), and hence we do not expect the surface free energy of a supersaturated paracetamol solution to deviate significantly from the surface free energy of pure water. In addition, the contact angle of a saturated solution of paracetamol does not differ significantly from the contact angle of pure water, except for the {110}-face (see Table 3). Furthermore, the supersaturation level has not been found to strongly influence the degree of agglomeration.[2] Hence, the fact that crystallization takes place in a supersaturated solution, and not in a pure solvent, is not believed to strongly alter the crystal–crystal interactions.

In the previous work,[1,2] the trend observed was a decrease in the degree of agglomeration with increasing solvent polarity (E_T), and the E_T-value was interpreted as a measure of the hydrogen bonding ability of the solvent. Figure 9 makes the corresponding presentation of the results of the present work. The agglomeration degree is given by the fraction of the particles having a C/A number less than 2. According to Figure 9, the agglomeration degree decreases with increasing solvent polarity, even though the correlation is somewhat scattered at E_T-values below 0.5 (crystallization in ethyl acetate, methyl ethyl ketone, acetonitrile, and acetone). The scatter around the correlation, is reflected in the correlation coefficient value (0.80), and is probably partly due to the rather rough measure of the degree of agglomeration—a specific fraction of the C/A number distribution of a sample. Since the shape of the C/A number distribution differ slightly depending on the solvent (Figure 3), this measure is a simplification. If the degree of agglomeration is described by the median C/A number of each sample a similar correlation is obtained.

Figure 10 presents the change in adhesion free energy with solvent polarity. As can be seen, despite scatter in the calculated free energy of adhesion for each solvent, and especially for water (E_T = 1.000), the free energy of adhesion overall correlates to the solvent polarity. The polarity index is an empirical parameter which describes the interaction of the solvent molecule with the phenoxide group in the pyridinium-*N*-phenoxide betaine dye as observed in the UV/vis spectrum.[22] The free energy of adhesion is a measure of the molecular interaction at the crystal–solvent interface, and in the case of paracetamol, exhibiting a rather similar surface chemistry of different crystal faces, it correlates to the solvent polarity. Hence, for organic crystals where the surface chemistry of different faces differs more substantially the adhesion free energy analysis of various pairs of faces opens up for a better prediction of the agglomeration behavior than the solvent polarity.

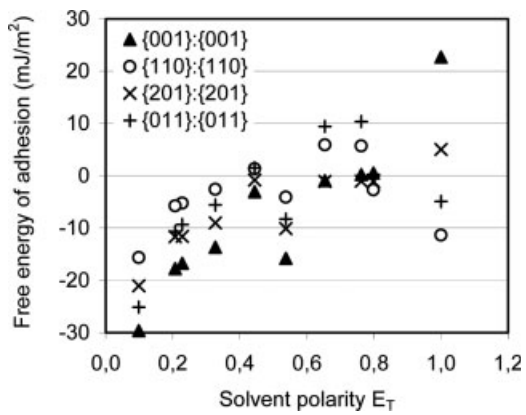

Figure 10. Change in adhesion free energy with solvent polarity (Tables 2 and 4).

Importance of crystal shape

As can be seen in Figure 6a, there is a large spread from negative (attractive) to positive (repulsive) values in the calculated adhesion free energy of different face combinations in water. Hence, the relative surface areas, which change with the crystal shape, are expected to become important for the degree of agglomeration in water. The shape of a paracetamol crystal which has grown in water changes with the supersaturation of the solution. When the supersaturation changes from low to high the crystal exhibits a change from an elongated columnar to a plate-like habit. Ristic et al.[27] have shown that the relative morphological importance of the {110}-face decreases, and that of the {001}-face increases with increased supersaturation due to change in the growth mechanism of the {110}-face with supersaturation. It is assumed that the actual contact at particle collision in an agitated crystallizer will vary quite randomly, and depending on the shape certain contacts will be favored. In the present work, the seeds grown from a highly supersaturated water solution are flat and tabular with large {001}-faces (Figure 1). Still after 4-min crystallization in water, the crystals are very little changed in their morphology (Figure 2a). This means that the {001}-faces are morphologically dominant and represent more than 50% of the total crystal surface area during the crystallization/agglomeration in water. Consequently, the suggested high relative morphological importance of the {001}-faces, and the values of the adhesion free energy when the {001}-face is involved (Figure 6a), can explain the observation of essentially no agglomeration in water. At the same time the seeds produced in water are to some extent agglomerated (C/A $<$ 2 = 67%), possibly as a result of strong attractive faces interactions, however, between faces having less relative morphological importance. Worth mentioning, we have tried to identify the actual crystallographic planes that are attached to one another in the agglomerates, however, so far without success.

It is interesting to notice the small changes in the crystal morphology after 4-min crystallization, for example, in ethyl acetate and methanol (see Figure 2). By X-ray diffractometry it is established that crystals grown in ethyl acetate (E_T = 0.228) do not expose the {110}-face and are therefore columnar in habit, and crystals grown in methanol (E_T = 0.762) are rhombic in habit due to an increased relative importance of the {110}-faces. This is in accordance with observations by Green and Meenan,[32] suggesting the relative importance of the {110}-face to increase with solvent polarity (E_T). However, as can be seen in Figure 6, the variation in the adhesion free energy of different combinations of crystal surfaces in ethyl acetate and methanol is much less than in water. Consequently, the agglomeration behavior is expected to be much less dependent on the crystal shape in ethyl acetate and methanol than in water. Still, for other organic crystals where the surface chemistry of different faces differs more than for paracetamol, the influence of the solvent on the crystal shape could be important for the agglomeration behavior.

Fluid mechanical conditions

In earlier crystallization experiments in acetone the degree of agglomeration gradually decreased with increased agitation rate from 400 to 600 rpm[2], beyond which the agglomeration degree was low and close to that of the seeds. The results suggest that at these agitation rates the particles are exposed to disruptive forces because of the agitation that are comparable in magnitude to the adhesion forces. In turbulent flow, the random fluid motions, also referred to as eddies, give rise to irregular fluid velocity gradients that may act to disrupt aggregates of crystals. The fluid–particle interactions in turbulent flow depend on the relative size of eddies and particles. The added seed crystals (90–125 μm) are larger than or in the size range of the Kolmogorov microscale, i.e. the smallest eddies in the flow (see Table 1). This means that particles in the experiments are influenced by normal pressure stresses that are caused by the relative velocity fluctuations between points in the close vicinity of the particle surface. The most common equation for describing the disruptive normal pressure stress on particles or droplets in a stirred tank is (e.g. Blandin et al.[33])

$$\tau_n = \frac{\rho \overline{u^2}}{2} \tag{11}$$

where $\overline{u^2}$ is the mean-square fluid velocity fluctuation and is given by

$$\overline{u^2} = 2(\varepsilon d)^{2/3} \tag{12}$$

According to this equation, the particle disruption is governed by the turbulence energy dissipation rate ε and the particle size d. In case of agglomeration, Mersmann[24] suggests the agglomerate breakage to take place when the shear stress of the liquid exceeds the agglomerate strength. The maximum turbulent shear stress is found in the impeller discharge stream and can be estimated by the following equation

$$\tau_s \approx 0.03 N_P \rho (\pi N D)^2 \tag{13}$$

Multiplying Eq. 11 or 13 with the cross-sectional area of a particle consisting of two crystals (approximated to be spherical with a diameter $d = 100$ μm), the disruptive force acting on the particle becomes

$$F_{dis} \approx \tau \frac{\pi d^2}{4} \tag{14}$$

As long as the adhesion forces are stronger than the disruptive fluid mechanical forces ($F_{adh} > F_{dis}$) the crystals may stay together and crystalline bridges can form between the crystals. The adhesion force between two crystals in a liquid can be estimated from Derjaguin's approximation for two identical spheres (100 μm in diameter):

$$F_{adh} = \frac{\pi d}{2} \Delta G_{SLS} \tag{15}$$

Figure 11 gives a comparison of the fluid mechanical forces at 400–800 rpm and the strongest adhesion force in methyl ethyl ketone (see Figure 6d, {001}:{001}). Methyl ethyl ketone is selected as an example since the surface free energy parameters for acetone are not available and hence the corresponding adhesion forces cannot be calculated. The fluid mechanical forces have been calculated for a maximum energy dissipation rate being 10 times the average value at each particular agitation rate ($N_p = 0.4$, Mersmann[24]). As can be seen in Figure 11, the calculated fluid mechanical forces using Eqs. 11 and 13 are two to three orders of magnitude lower than the maximum adhesion force.

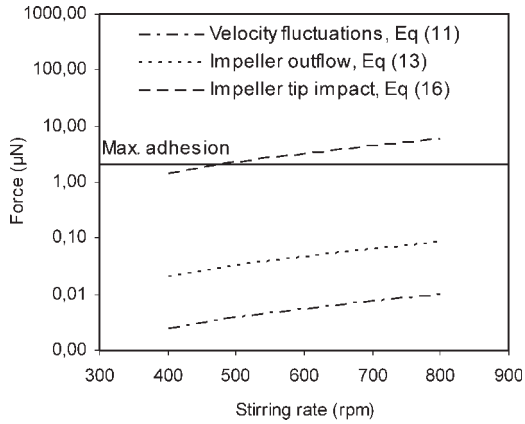

Figure 11. Change in disruptive forces with agitation rate in methyl ethyl ketone.

The horizontal line represents the maximum adhesion force (the interaction of two {001}-faces).

In our calculations all particles (individual crystals and aggregates) are considered to be spherical, which of course is an oversimplification. For example, Mullins et al.[34] report of significantly smaller adhesion forces for flakes and irregular shaped particles than for spheres with similar characteristic dimensions (5 μm). In addition, surface asperities (roughness) can significantly influence the adhesion forces. The strength of the Lifshitz–van der Waals (LW) interaction decay with increasing distance to the second order and the strength in the acid–base (AB) interaction decay exponentially with increasing distance.[6] Within a distance of $\sim$30 Å, which is very much smaller than the microscopic surface roughness observed on the slowly grown crystal shown in Figure 7, the free energy of adhesion falls off to zero. Crystals in a crystallizer grow faster, are much rougher, and exhibit more defects. Hence, it is possible that the absolute values of the adhesion forces are lower than estimated above.

Another point is that the hydrodynamics of an agitated tank are very complex and exhibit a very significant spatial variation. The local energy dissipation rate varies by at least two orders of magnitude.[35] However, perhaps more important is the possibility of the particles actually impacting with the agitator blades. The impact force induced by the impeller tip can be estimated as:

$$F_{imp} = ma \approx \rho_s \left(\frac{\pi d^3}{6}\right) \frac{u_{tip}^2}{2 l_a} = \frac{\rho_s \pi d^3 (N \pi D)^2}{12 l_a} \tag{16}$$

where the acceleration distance l_a is particularly difficult to estimate because the detailed conditions of the impact are complex. For a proper estimation of the force exerted on the particle, the mechanics of the impact need to be analyzed and the deformation and breakage behavior of the agglomerate

must be accounted for. However, it turns out that the impact forces are quite close to the adhesion forces (see Figure 11) when the acceleration distance is given the approximate size of the colliding particle ($l_a = d = 100$ μm). Hence, disruption by impeller collision may provide one possible explanation for the influence of the agitation rate and for the balance between adhesion and disruption. The possibility of smaller acceleration distances indicates the possibility of impact forces being able to break also crystalline bridges.

Conclusions

In well-defined isothermal crystallization/agglomeration experiments, with seeding and constant supersaturation, it is found that the degree of agglomeration of paracetamol is substantial in acetone, in particular, but also in acetonitrile and methyl ethyl ketone. In water, methanol, and ethanol the degree of agglomeration is fairly low. The degree of agglomeration is reasonably well correlated to the polarity of the solvent.

By contact angle measurements and the Lifshitz–van der Waals acid–base theory, the surface free energy of four different faces of well-grown paracetamol crystals have been determined to be in the range 50–57 mJ/m^2. All faces are found to possess a strong negative polar component, i.e. the surfaces are strongly electron-donating (H-bond-accepting). However, this is not completely understandable from the molecular arrangement of the faces and it leads to interfacial energy values that sometimes are unrealistic for the present systems. A cause for this is perhaps the assumed equal polar component values of water that underlies the entire scale of polar surface free energy parameter values.

From surface and interfacial free energy values, crystal–crystal adhesion free energies for different faces in different solvents are calculated. These adhesion forces are much stronger than the forces exerted by the fluid turbulence, but are comparable to the impact force exerted on particles colliding with the impeller tip.

The results show that there is a correlation between the degree of agglomeration and an independent assessment of the free energy of adhesion. Hence, even though the reliability of the interfacial energy values is somewhat unclear, this trend lends support to the hypothesis that the influence of the solvent on the degree of agglomeration of paracetamol can be explained to an important extent as being the result of differences in the free energy of adhesion. This also provides for a mechanistic explanation for the correlation to the solvent polarity.

Acknowledgments

The authors are grateful to Dr. Eva Blomberg and Prof. Per Claesson at the Surface Force Group, Dept. of Chemistry, KTH/YKI, for their support and kind permission to use the goniometer equipment. Dr. Andreas Fischer at the Div. of Inorganic Chemistry, Dept. of Chemistry, KTH, is acknowledged for identification of faces with single-crystal X-ray diffractometry.

Notation

d = particle diameter, m
D = impeller diameter, m
E_T = normalized solvent polarity
F = force, N
ΔG = free energy of interaction, mJ/m^2
l_a = acceleration distance, m
N = stirring rate, rps
N_p = power number
Re = Reynolds number
S = supersaturation
u = velocity, m/s
$\overline{u^2}$ = mean square fluid velocity fluctuation, m^2/s^2
V = volume of tank, m^3
γ = surface free energy or interfacial free energy, mJ/m^2
ε = energy dissipation rate, W/kg
θ = contact angle, $^\circ$
λ_K = Kolmogorov microscale, m
ν = kinematic viscosity, m^2/s
ρ = density, kg/m^3
τ = stress, N/m^2

Subscripts

S = solid
L = liquid

Superscripts

AB = Lewis acid–base
LW = Lifshitz–van der Waals
$+$ = electron-acceptor
$-$ = electron-donor

Literature Cited

1. Ålander EM, Uusi-Penttilä MS, Rasmuson ÅC. Agglomeration of paracetamol during crystallization in pure and mixed solvents. *Ind Eng Chem Res.* 2004;43:629–637.
2. Ålander EM, Rasmuson ÅC. On the mechanisms of crystal agglomeration of paracetamol in acetone-water mixtures. *Ind Eng Chem Res.* 2005;44:5788–5794.
3. Ålander EM, Uusi-Penttilä MS, Rasmuson ÅC. Characterization of paracetamol agglomerates by image analysis and strength measurement. *Powder Technol.* 2003;130:298–306.
4. Wu W, Nancollas GH. Determination of interfacial tension from crystallization and dissolution data: a comparison with other methods. *Adv Colloid Interface Sci.* 1999;79:229–279.
5. van Oss CJ, Good RJ, Chaudhury MK. Additive and non-additive surface-tension components and the interpretation of contact angles. *Langmuir.* 1988;4:884–891.
6. Clint JH. Adhesion and components of solid surface energies. *Curr Opin Colloid Interface Sci.* 2001;6:28–33.
7. Bramley AS, Hounslow MJ, Newman R, Peterson WR, Pogessi C. The role of solution composition on aggregation during precipitation. *Chem Eng Res Des A.* 1997;75:119–124.
8. van Oss CJ. *Interfacial Forces in Aqueous Media*. New York: Marcel Dekker, 1994.
9. Clear SC, Nealey PF. Chemical force microscopy study of adhesion and friction between surfaces functionalized with self-assembled monolayers and immersed in solvents. *J Colloid Interface Sci.* 1999; 213:238–250.
10. Kokkoli E, Zukoski CF. Effect of solvents on interactions between hydrophobic self-assembled monolayers. *J Colloid Interface Sci.* 1999;209:60–65.
11. Muster TH, Prestidge CA. Face specific surface properties of pharmaceutical crystals. *J Pharm Sci.* 2001;91:1432–1444.
12. Freitas AM, Sharma MM. Effect of surface hydrophobicity on the hydrodynamic detachment of particles from surfaces. *Langmuir.* 1999;15:2466–2476.
13. Freitas AM, Sharma MM. Detachment of particles from surfaces: an AFM study. *J Colloid Interface Sci.* 2001;233:73–82.
14. Kwok DY. The usefulness of the Lifshitz-van der Waals/acid-base approach for surface tension components and interfacial tensions. *Colloids Surf A: Physicochem Eng Aspects.* 1999;156:191–200.
15. Makkonen L. On the methods to determine surface energies. *Langmuir.* 2000;16:7669–7672.

16. Della Volpe C, Maniglio D, Brugnara M, Siboni S, Morra M. The solid surface free energy calculation I. In defense of the multicomponent approach. *J Colloid Interface Sci*. 2004;271:434–453.
17. Hollander A. On the selection of test liquids for the evaluation of acid-base properties of solid surfaces by contact angle goniometry. *J Colloid Interface Sci*. 1995;169:493–496.
18. Della Volpe C, Siboni S. Some reflections on acid-base solid surface free energy theories. *J Colloid Interface Sci*. 1997;195:121–136.
19. Della Volpe C, Siboni S. Acid-base surface free energies of solids and the definition of scales in the Good-van Oss-Chaudhury theory. *J Adhes Sci Technol*. 2000;14:235–272.
20. Lee L-H. The unified Lewis acid-base approach to adhesion and solvation at the liquid-polymer interface. *J Adhes* 2001;76:163–183.
21. van Oss CJ. Acid-base interfacial interactions in aqueous media. *Colloids Surf A: Physicochem Eng Aspects*. 1993;78:1–49.
22. Reichardt C. *Solvents and Solvent Effects in Organic Chemistry*, 3rd ed. Weinheim: Wiley-VCH, 2003.
23. Granberg RA, Rasmuson ÅC. Solubility of paracetamol in pure solvents. *J Chem Eng Data*. 1999;44:1391–1395.
24. Mersmann A. *Crystallization Technology Handbook*, 2nd ed. New York: Marcel Dekker, 2001.
25. Naumov DY, Vasilchenko MA, Howard JAK. The monoclinic form of acetaminophen at 150K. *Acta Crystallogr C*. 1998;54:653–655.
26. Granberg RA, Ducreux C, Gracin S, Rasmuson ÅC. Primary nucleation of paracetamol in acetone-water mixtures. *Chem Eng Sci*. 2001;56:2305–2313.
27. Ristic RI, Finnie S, Sheen DB, Sherwood JN. Macro- and micromorphology of monoclinic paracetamol grown from pure aqueous solution. *J Phys Chem B*. 2001;105:9057–9066.
28. Morra M, Occhiello E, Garbassi F. Knowledge about polymer surfaces from contact angle measurements. *Adv Colloid Interface Sci*. 1990;32:79–116.
29. Gracin S, Brinck T, Rasmuson ÅC. Prediction of solubility of solid organic compounds in solvents by UNIFAC. *Ind Eng Chem Res*. 2002;41:5114–5124.
30. Granberg RA, Gracin S, Rasmuson ÅC. Crystal growth rates of paracetamol in binary and ternary mixtures of water + acetone + toluene. *AIChE J*. 2005;51:2441–2456.
31. Granberg RA. *The Influence of Solvent Composition on Crystallization of Paracetamol*, Doctorial Thesis. Stockholm: Department of Chemical Engineering and Technology, Royal Institute of Technology, 2000.
32. Green DA, Meenan P. Acetaminophen crystal habit: solvent effect. In: Myerson AS, Green DA, Meenan P, editor. *Crystal Growth of Organic Materials*. Washington, DC: American Chemical Society, 1996:78–84.
33. Blandin AF, Mangin D, Subero-Couroyer C, Rivoire A, Klein JP, Bossoutrot JM. Modelling of agglomeration in suspension: application to salicylic acid microparticles. *Powder Technol*. 2005;156:19–33.
34. Mullins ME, Michaels LP, Menon V, Locke B, Ranade MB. Effect of geometry on particle adhesion. *Aerosol Sci Technol*. 1992;17:105–118.
35. Pettersson M, Rasmuson ÅC. Hydrodynamics of suspensions agitated by a pitched-blade turbine. *AIChE J*. 1998;44:513–527.

Manuscript received Jun. 12, 2007.